Original Research Paper

Volume-10 | Issue-2 | February - 2020 | PRINT ISSN No. 2249 - 555X | DOI : 10.36106/ijar

Rheumatology

USE OF EX VIVO-GENERATED CARTILAGE DERIVED FROM HUMAN BONE MARROW MESENCHYMAL STEM CELLS EXPANDED IN MEDIUM SUPPLEMENTED WITH FGF2 IN TREATING SURGICALLY-INDUCED CHONDRAL DEFECTS IN ATHYMIC RAT KNEE: A STEP TOWARDS TREATING HUMAN OSTEOARTHRITIS

Subhash C. Juneja

Research Associate, The Arthritis Program, Krembil Research Institute, Toronto Western Hospital, Krembil Research Institute, University Health Network, Toronto, Canada M5T 2S8

ABSTRACT

Aim and objectives: The degeneration of articular cartilage in joints leads to osteoarthritis that in turn causes life long pain in joints and, impair the mobility of patients in many cases. The available remedies to treat osteoarthritis are the drugs to reduce the pain, and or joint replacement. The success of second option is not always easy and comes with a heavy price tag and with post-surgical complication, in some cases. The resurfacing of knee joint or hip joint cartilage defects with bone marrow-derived mesenchymal stem cells (MSCs) can be a promising opportunity for joint cartilage repair to treat osteoarthritis. The long-term advantage of this research is that transplantation of cartilage tissue generated *ex vivo* from MSCs isolated from bone marrow aspirated from the same patient to treat the patient's knee or hip osteoarthritis, *i.e*., autologous transplantation that assures low rejection rate. Since MSCs can be expanded through multiple passages, the cell source can be enormous and the cells can be frozen in liquid nitrogen for long time to coordinate the timing of patient's treatment. To further enhance the MSCs chondrogenic differentiation efficiency and transplantability of derived chondrogenic tissue, MSCs may be pre-treated with certain growth factors, FGF2, or FGF2+WNT3A before chondrogenesis begins.

Methods: MSCs were isolated from human bone marrow and were characterized as described earlier. Bone marrow was aspirated from patients undergoing total knee arthroplasty or total hip arthroplasty. Cartilages were generated *ex vivo* from chondrogenic differentiation of MSCs. Before chondrogenesis began, MSCs were expanded in MSCs medium only (abbr. MSCs_MO group) or MSCs medium containing FGF2 (abbr. MSCs_FGF2 group) or MSCs_FGF2+WNT3A (abbr. MSCs_FGF2+WNT3A group) for one passage. Expanded MSCs were than placed for chondrogenesis for 4 weeks in complete chondrogenesis medium (CCM) on COL II-coated transwell inserts in 24-well plates at high density. CCM was changed every 48hr. Cartilages were characterized by special stainings and immunohistochemistry on paraffin-embedded sections, and transmission electron microscopy (TEM) as described earlier (Juneja *et al*., 2016). Cartilage from each group was transplanted in two femoral trochlear defects created surgically in the right knee of athymic nude rat (n=7 rat in each group). Knee defects transplanted with fibrin glue served as control. At 8-weeks post surgery, rats were sacrificed, knee decalcified, paraffin-embedded sections of knee were assessed for repair of knee defects using Safranin O staining and COL II immunostaining.

Results: *Ex vivo*-generated cartilages differed in their properties. Hardness of cartilage was in this order in cartilage groups: MSCs_FGF2+WNT3A > MSCs_FGF2 > MSCs_MO. Thickness of cartilage was in this order: MSCs_FGF2+WNT3A > MSCs_FGF2 > MSCs_MO ($P<0.001$). paragraphs in cartilage were in this order: MSCs_FGF2+WNT3A > MSCs_FGF2 > MSCs_MO as determined by toluidine blue staining ($P<0.001$) as well as by Safranin O staining. All the groups of cartilages showed the presence of positive chondrogenic markers (COL II, COL VI, aggrecan and lubricin) and absence of hypertrophic chondrocyte marker (COL X) as shown by immunohistochemistry. There was no mineralization and apoptosis in cartilages as shown by von Kossa and apoptosis tunnel assay, respectively. TEM showed that chondrocytes in cartilages were from 'best to worst' in this order: MSCs_FGF2 > MSCs_FGF2+WNT3A > MSCs_MO. Chondrocyte quality was assessed by the presence of number of lipid droplets and ovalness of the chondrocyte's nucleus. More the number of lipid droplets in chondrocyte, worst the quality of chondrocyte. More the indented and lobulated nucleus in chondrocyte, worst the chondrocyte. More oval chondrocyte was considered as best chondrocyte. The transplantation success of cartilages was in order from 'best to worst': MSCs_FGF2 > MSCs_FGF2+WNT3A > MSCs_MO groups. Cartilage transplantation success was based on COL II staining and Safranin O staining of defects region.

Conclusion: *Ex vivo*-generated cartilage, differentiated from MSCs derived from human bone marrow, was able to repair induced-chondral defects in athymic nude rat knee. Using this method, human osteoarthritis can be treated using patient's own bone marrow derived MSCs.

KEYWORDS : Mesenchymal stem cells, Chondrocyte, FGF2, WNT3A, Chondral defect, Osteoarthritis, Bone marrow, Athymic rat knee, Lipid droplets

INTRODUCTION

Osteoarthritis (OA) is the common form of arthritis in adults and is the leading cause of disability in elderly patients (Yelin, 2003). In United States alone, over 27 million adults suffer from osteoarthritis leading to a substantial health and financial burden (Lawrence *et al*., 2008; Chu *et al*., 2010). OA is a degenerative process affecting peripheral joints and the spine. According to OA definition, it is characterized by a set of radiographic findings associated with symptoms of non-inflammatory arthritis. OA is likely the ultimate pathway of many small and large insults to the joints, whose connective tissues have limited capacity to repair. It is obvious that genetic, mechanical, and even inflammatory events contribute to the development of OA. While OA is recognized by progressive damage to the articular cartilage, other tissues such as bone, tendon, enthesis, ligament, meniscus and muscle may participate in OA pathogenesis. It is not clear if pain reduction should be the primary target of therapy, or if restoration of normal articular cartilage would be a better choice.

Currently, no drugs are available that can treat cartilage defects effectively. Cartilage defects lead to the development of OA, the condition can be managed by multiple ways including physiotherapy, pharmacotherapy and or joint replacement surgery (Alshami, 2014). However, several surgical interventions may be performed in order to prevent progression towards OA (Tsumaki *et al*., 2015). Current procedures include arthroscopic lavage and debridement, microfracture induction, and autologous chondrocyte transplantation. Although these procedures have been proposed to restore normal joint function and minimize further damage still they do not offer a long-term treatment (Makris *et al*., 2015). There is a need to develop regenerative approaches to restore articular cartilage permanently.

Both adult mesenchymal stem cells (MSCs) and induced pluripotent stem cells (iPSCs) are promising stem cell source to achieve cartilage regeneration (Jia *et al*., 2018; Mak *et al*., 2016; Gardner *et al*., 2019). However, the use of adult MSCs still faces some challenges such as cell senescence and donor variability (Wagner *et al*., 2008; Surdo and Bauer, 2012; Vono *et al*., 2018). We have taken this challenge to plan experiment so that current problem of using MSCs to repair osteoarthritis can be better resolved. The current study was designed to repair knee femoral chondral defects in rats. *Ex vivo* generated cartilages differentiated from MSCs were transplanted into the knee defects for the integration with the host cartilage to assess the repair of host cartilage simulating the process of repair of human OA defects. The study will be applicable to treat human OA using the patient's own bone marrow derived MSCs.

Aims and objectives:

The aim of the study was to discover a reliable method to treat osteoarthritis using human bone marrow derived MSCs-differentiated cartilage tissue using rat model. The model can be used in human to treat OA using patient's own bone marrow-derived MSCs-differentiated cartilage tissue.

MATERIALS AND METHODS

Bone marrow was aspirated from patients undergoing knee and hip replacement surgery from Toronto Western Hospital, Toronto, Canada. MSCs were prepared from bone marrow and characterized as described earlier (Juneja *et al*., 2016). MSCs at passage 3 were expanded for one additional passage in MSCs medium only (abbr. MSCs_MO group) or MSCs medium containing FGF2 (abbr. MSCs_FGF2 group) or FGF2+WNT3A (abbr. MSCs_ FGF2+ WNT3A group) for one passage. The expanded MSCs were placed on collagen-coated inserts in 24 well plates in complete chondrogenesis medium (CCM). At 4 weeks, cartilages were obtained, characterized and transplanted in knee defects created surgically in athymic rats. Rat knee defects were assessed at 8-weeks post-surgery for the integration of *ex vivo* generated cartilage. The details of methods are described as below in various steps.

Preparation of COL II-coated cell culture transwell membrane inserts:

Transwell membrane of hydrophilic PTFE cell culture inserts (pore size 0.4µm, Millicell® inserts, for 24-well plate, (PICM01250, Millipore) were coated with type II collagen (Col-II, Type II collagen from chicken sternal cartilage, C9301, Sigma-Aldrich). A stock solution of COL II (2mg/ml) was prepared in 0.1 M acetic acid. The mixture was swirled gently, and placed at 4˚C for 4h to dissolve and than stored at 4˚C till use. A working solution of COL II (0.5mg/ml) was prepared with dH_2O at room temperature (RT). Cell culture inserts were positioned in 24-well plate (3526, Costar® Corning). A total of 175µl COL II working solution was dispensed in each insert. The plate carrying inserts was incubated overnight at RT in a biosafety flow hood. Extra fluid was aspirated from the inserts and transmembrane was allowed to dry for 2h. Inserts were exposed to UV light for 20 min in the biosafety flow hood. Prior to use, each inert was given a quick rinse with 200µl CCM to remove any residual acetic acid.

Isolation of MSCs from bone marrow aspirated from patients undergoing total knee arthroplasty (TKA) or total knee arthroplasty (THA):

The research study protocol was approved by Research Ethics Board (REB), University Health Network, Toronto, Canada. The bone marrow was retrieved from patients (age, 55-65 years) undergoing TKA or THA with their prior consent. Briefly, bone marrow was aspirated by an orthopaedic surgeon from patient's femur cavity by gliding a Baron suction needle (13") attached to the specimen trap (BW406, Cardinal Health) containing 2000 IU (1000IU/ml) heparin (DIN-453811, Heparin Leo®, Leo Pharma) and the trap, in turn, connected to suction system. The isolation and characterization of MSCs has been described in detail elsewhere (Juneja *et al*., 2016). The trap containing bone marrow was transported to the laboratory at RT within 1 hour. The marrow was diluted with 5 volumes of Ca^{++}-mg^{++}-free Dulbecco's Phosphate Buffered Saline (D8537, Sigma-Aldrich) and 1 volume of 2mM EDTA (AM9260G, EDTA, 0.5M, pH 8.0, Life Technologies) followed by shaking the contents of the container (trap) 10-15 times, filtered through a wide-holed iron mesh to remove any fibrotic tissue and bone particles, and finally centrifuged at 300g for 10 min in 50ml tubes. The upper fat layer in the centrifuge tube was discarded. The large middle layer of supernatant was carefully aspirated and discarded. The bottom red colored pellet was resuspended in 35ml D-PBS (D8662, Dulbecco's Phosphate-Buffered saline, Sigma-Aldrich) containing 2% bovine serum albumin (A9418, Sigma-Aldrich) and centrifuged at 300g for 5 min. This step was repeated once to wash off residual EDTA. Finally the pellet was resuspended in D-PBS with 2% BSA (in a volume equal to original volume of bone marrow). A total of 5-7 ml of pellet suspension was layered on the top of 4ml Ficoll-Paque Plus (17-1440-02, GE Healthcare) in 15-ml centrifuge tubes. The tubes were centrifuged at 435g for 30min to achieve gradients. The middle gradient layer rich in mononuclear cells (MNCs) was carefully removed, washed in MSCs medium by centrifugation. Thirty million MNCs were plated per 175cm^2 tissue culture flask (353112, BD Falcon) containing 40ml MSCs-medium in humidified 5% CO_2 incubator at 37ºC. The MSCs-medium constituted of DMEM with low glucose (11054, Gibco® by Life Technologies), 1% GlutaMAX™ CTS™ (100x, A12860, Gibco® by Life Technologies) and 1% Penicillin-Streptomycin (P4333, Sigma-Aldrich) supplemented with 10% FBS (SH30070, Fetal Bovine Serum, HyClone, Thermo Fisher Scientific). MSCs colonies were detected at 48-96h. Media was changed every third day. Once 70%-80% confluency was achieved, the dishes were trypsinized with TrypLE™ Select CTS™ (A12859, Gibco® by Life Technologies), and placed in culture for next passage.

MSCs were frozen at passage 2 in freezing medium constituted of 10% DMSO (D2650, Sigma-Aldrich), 50% FBS, 40% MSCs-medium without FBS. The cryopure tubes (72.377.002, Sarstedt) were placed in Mr. Frosty™ freezing container (5100-0001, Thermo Scientific) that was placed at -70˚C for 24h and than tubes were transferred to liquid nitrogen. MSCs were grown to passage 3 and characterized for their specific positive and negative markers by immunofluorescence by a kit (SCR067, Human Mesenchymal Stem Cell Characterization Kit, Millipore). Positive cell markers include antibodies directed against cell-surface molecules present on MSCs: CD44, CD90, STRO-1, and CD146 and negative markers: markers specific to hematopoietic cell surface, CD14 (present on leukocytes) and CD19 (present on B-lymphocytes). Further MSCs at passage 3 were assessed by their differentiation ability for osteogenesis, chondrogenesis and adipogenesis using kits (A10072-01, A10071-01 and A10070-01 respectively, StemPro®, Life Technologies). MSCs characterization is described earlier (Juneja *et al*., 2016).

Expansion of MSCs in the presence of FGF2 or FGF2+WNT3A for one passage:

Routinely, frozen MSCs tubes at passage 2 were thawed in 37˚C water bath and grown for one more passage. At passage 3, MSCs were plated in 175cm^2 tissue culture flask either in MSCs medium only (MSCs_MO) or in MSCs-medium containing 10ng/ml FGF2 (recombinant human FGF basic, Cat No, 233-FB, R&D Systems) (MSCs_FGF2) or in MSCs-medium containing 10ng/ml FGF2 and 100ng/ml WNT3A (recombinant human WNT-3A, Cat no. 5036-WN, R & D systems) (MSCs_FGF2+WNT3A). At 96h post-plating, MSCs monolayers were trypsinized, washed once with its respective spent medium, cells were placed in CCM with MSCs; concentration of each group was adjusted to $4x10^6$ cells/ml in CCM.

Complete chondrogenesis medium (CCM):

CCM was prepared by mixing 'incomplete chondrogenesis medium' (Table 1) and TGFβ3 at a concentration of 10ng/ml. TGFβ3 powder (Recombinant human TGF-beta 3, Cat no. 243-B3, R&D Systems) was reconstituted as stock solution and aliquoted as per manufacturer's instructions. The stock solution (20µg/µl) was stored in 25µl aliquots at -70˚C. CCM was prepared by adding 500ng TGFβ3 (25µl stock solution) to 100 ml incomplete chondrogenesis medium. The CCM medium was used within 2 days.

Table 1. Composition of 'incomplete chondrogenesis medium'.

Reagent	Cat. No.	Stock solution	For 500 ml medium, Mix & filter sterilize	Final conc.
DMEM w high glucose, 1x	D5671 (Sigma-Aldrich)		474.5ml	1x
L-Ascorbic Acid 2-phosphate Trisodium Salt	323-44822 Wako (CEDARLANE® Laboratories)	5mg/ml in dH_2O (4˚C)	5ml	50µg/ml
L-Proline	P5607 (Sigma-Aldrich)	50mg/ml in dH_2O (4˚C)	500µl	50µg/ml
Insulin-Transferrin-Selenium-Sodium Pyruvate (ITS-A) (100x)	51300-044 (Gibco® by Life Technologies)		5ml	1x
Sodium pyruvate (100mM)	11360-070 (Gibco® by Life Technologies)		5ml	1mM

Penicillin-Streptomycin (10,000 U/ml)	15140-122 (Gibco® by Life Technologies)		5ml	100 U/ml
GlutaMAX™ Supplement (100x)	35050-061 (Gibco® by Life Technologies)		5ml	1x
Linoleic acid (1gm/ml)	L1012 (Sigma-Aldrich)	Dilute 5µl L1012 (1gm/ml) to 50µl in dH2O before use] and label it as 'Stock solution' (100µg/µl)	26.65µl 'Stock solution'	5.33 µg/ml
Dexamethasone (MW: 392.46)	D4902, (Sigma-Aldrich)	*Dissolve 25mg D4902 in 6.37ml ethanol and store at -20˚C). Label it as 'Solution-A' (10mM) *Dilute 100µl 'Solution-A' to 1ml in dH_2O before use. Label it as 'Solution-B' (1mM):	50µl 'Solution-B'	100nM

Chondrogenesis:
A high density MSCs ($2x10^6$ in 0.5ml CCM) were plated at the center of Col-II-coated inserts placed in a 24-well plate. The cells were allowed to settle at 1g after placing plate in a humidified CO_2 incubator at 37ºC. After 2h, each insert was added additional 1.3ml CCM. Each plate was inspected for any air bubble at the bottom of the insert under the stereomicroscope. Air bubble was removed by lifting the insert up with sterile forceps. CCM was replaced every 48h until day 28. The inserts were removed and the transmembrane along with the generated cartilage was cut along the periphery with a blade (Disposable scalpel no. 11, M92-11, Almedic). Cartilages were transferred to freshly diluted 4% paraformaldehyde (RT15700, EM Sciences) for overnight at 4ºC. The cartilages were washed once in PBS, transferred to 70% ethanol and processed for paraffin blocks. Four µm paraffin sections were cut along the diameter of circular disc-shaped cartilage.

Safranin O staining:
Proteoglycans were localized in the *ex vivo*-generated cartilage sections by Safranin O staining. Paraffin sections were deparaffinized in xylene (3x, 3min), dehydrated by treating with decreasing concentrations of ethanol [100%, 95%, 70%, 0% (dH_2O), 2x, 3min each] and finally placed in dH_2O. The sections were stained in Weigert's iron hematoxylin (5min), rinsed in changes of dH_2O till leaching of blue coloration stopped. Sections were differentiated in 1% acid-alcohol (2secs), rinsed in dH_2O (3x), treated with 0.02% Fast Green (1min), 1% acetic acid (30secs) and 1% Safranin O (10 min). The sections were dehydrated in 95% ethanol (3x, 3min), 100% ethanol (2x, 2min), cleared in xylene (3x, 3min) and mounted in Permount™ mounting medium (17986, EM sciences).

Toluidine blue staining:
Proteoglycans were also assessed using Toluidine blue staining. Paraffin-embedded sections of *ex vivo*-generated cartilages were deparaffinized and hydrated as described earlier in the text. Hydrated slides were treated in sequence with: 0.01% acetic acid (1min), dH_2O (2 dips), freshly filtered 0.1% Toluidine blue (T161, Fisher Scientific) (35-45secs), dH_2O (3dips) and finally 2-3 dips of acetone. The sections were blot dried, air dried for 2 min, cleared in xylene and mounted using mounting medium as described before.

Masson's trichrome staining:
Presence of collagen was assessed using Masson's trichrome staining. Paraffin-embedded sections of *ex vivo*-generated cartilages were deparaffinized and hydrated as described earlier in the text. The hydrated slides were placed in pre-warmed 0.2% chromic acid at 60°C (5min), rinsed in tap H_2O (5x), stained in Weigert's iron hematoxylin (10min), washed in running tap H_2O (2-5min), differentiated in 1% acetic acid (1-2 dips), washed in running tap H_2O (2-5min), treated with 1% Biebrich Scarlet (AC402221000, Fisher Scientific) in acetic acid (1min), rinsed in running tap water (2min), treated with 5% Phoshotungstic Acid/Phosphomolybdic Acid (A237-100, A248-500, Fisher Scientific) for 1min, treated in 1% light green SF yellowish (P399-03, JT Baker) and differentiated in 1% acetic acid and rinsed in tap water (5 times). The slides were dehydrated and mounted as described before.

Picrosirius red staining:
This staining was used for localizing collagen in *ex vivo*-generated cartilages. Paraffin sections were deparaffinized and hydrated as described earlier. Hydrated sections were stained with picrosirius red stain kit as described in manufacturer's instructions manual (24901, Polysciences, Inc.). After staining, the sections were dehydrated and mounted as described before. Picrosirius red stain binds specifically to collagen fibrils of varying diameter. The mounted slides were viewed under light microscope using polarizing light to view the orientation of collagen fibrils.

von Kossa staining:
Mineralization in the tissue sections was assessed by NovaUltra von Kossa Stain Kit (IW3014, IHC World) following manufacturer's instructions. Tissue paraffin sections were deparaffinized and hydrated as described earlier in the text. Hydrated tissue sections were placed in silver nitrate solution, exposed to UV light for 1h in a clean glass Coplin jar, washed in changes of dH_2O (3x), rinsed once with sodium thiosulfate solution (1-2 min), washed once with dH_2O, counterstained with nuclear fast red (5min) and rinsed in dH2O. The sections were dehydrated and mounted as reported earlier.

Apoptosis:
Apoptosis in chondrocytes of *ex vivo*-generated cartilage sections was determined by using AopTag® Peroxidase *in Situ* Apoptosis Detection Kit (7100, Millipore) following manufacturer's instructions. During apoptosis, DNA fragmentation takes place and apoptotic bodies are rich in free OH^- ends. The kit is designed to label free OH^- ends by adding a mixture of digoxigenin-labeled and non-labled nucleotides in the presence of terminal deoxynucleotidyl transferase. The resulting oligomer added to apoptotic DNA fragment's ends allows the binding of anti-digoxigenin antibody conjugated to a peroxidase reporter molecule. The later is detected using peroxidase substrate diaminobenzidine (ImmPACT™ DAB Substrate, Sk-4105, Vector laboratories) which gives dark brown staining and can easily be viewed under light microscopy. Paraffin section of involuting mouse mammary gland at day-4 post parturition was used as a positive control.

Transmission electron microscopy (TEM):
The *ex vivo*-generated cartilages were fixed in universal buffer for 48h at 4˚C. The tissues were cut into smaller pieces, washed in Millonig's buffer (3x), post-fixed in 1% osmium tetroxide in 0.1 M sodium cacodylate (pH 7.4), washed again with Millonig's buffer (3x). Tissues were dehydrated in increasing concentrations of ethanol upto 100%, transferred to 100% acetone, infiltrated in acetone/epon (1:1), transferred in 100% epon and embedded in beam molds and polymerized for 2 days at 70˚C. Semi-thin sections at 1µm were cut for Toluidine blue staining for initial assessment. For TEM, 90˚A sections were cut. The grids were stained with uranyl acetate/lead citrate. The sections were examined using a JOEL JEM-1011 electron microscope at Hospital for Sick Children at Toronto, Canada.

Immunohistochemistry (IHC):
Ex vivo generated-cartilages were characterized by localizing positive specific antigens (COL II, COL VI, aggrecan and lubricin), and negative specific antigen (COL X) for articular cartilage by IHC. Slides with paraffin sections were heated at 58–60ºC for 60 min. The slides at RT were deparaffinized and hydrated as described earlier in the text. The hydrated sections went through antigen retrieval process as mentioned in the notes below Table 2. To avoid non-specific background due to the presence of endogenous peroxidase, pseudo peroxidase and alkaline phosphatase, hydrated sections were incubated with Dual Endogenous Enzyme Block (S-2003, Dako) for 10 minutes followed by a rinse with dH_2O. Sections were blocked with blocking buffer (PBS-T containing 2% BSA and 2% serum of species in which secondary antibody is raised) for 30 min at RT. Blocking buffer was replaced by primary antibody for 2 hours in a humidified chamber at RT or overnight at 4ºC. Step A or B was followed depending upon the antigen. Step A. For COL II, COL X, aggrecan and lubricin, the sections were washed with PBS-T (4x, 5min), treated with

blocking buffer for 30min, and incubated with secondary antibody (Table 2) for 30min. The sections were washed with PBS-T (4x, 5 min) and incubated with ABC reagent [ABC reagent was prepared 30 min before incubation (PK-6100, Elite ABC-HRP kit, Vector)] for 30 min. Step B. For COL VI, the sections were washed with PBS-T (4x, 5min), and treated with Streptavidin-HRP (diluted in PBS-T, ab7403, abcam) for 30min.

After following step A or B, sections were washed with PBS-T (2x, 3 min; 4x, dH_2O, 5min) and brown color was developed using DAB substrate. The sections were stained with Meyer's hematoxylin, washed, dehydrated, cleared, mounted, scanned, and photographed as described earlier. Positive control tissues were included as shown in Figures 4 and 5.

Table 2. Antibodies used in immunohistochemistry (IHC).

Antigen	Primary antibody	Secondary antibody
Type II collagen (COL II)	Mouse anti-COL II, monoclonal, II-II6B3, DSHB	Biotinylated horse anti-mouse IgG, rat adsorbed, BA-2001, Vector
Type X collagen (COL X)	Mouse anti-COL X, monoclonal, 2031501001, Quartett, GE	Same as above
Lubricin	Clone 9g3, MABT401 (Gift from Dr. George Jay)	Same as above
Aggrecan	Rabbit polyclonal to aggrecan, ab36861, abcam	Biotinylated horse anti-rabbit IgG, BA-1100, Vector
Type VI collagen (COL VI)	Rabbit polyclonal to COL VI (Biotin), ab6583, abcam	None

IHC Notes:
(i) Primary and secondary antibodies were diluted in blocking buffer.

(ii) Negative control was without primary antibody and with mouse IgG (for COL II, COL X, Lubricin) and with rabbit IgG, polyclonal (ab27478, abcam), for aggrecan and COL VI. Images of negative control sections are not shown in figures.

(iii) For antigen retrieval for COL II, COL X and aggrecan, the hydrated tissue sections were treated with pepsin (P-7000, Sigma-Aldrich; 4mg/mL in 0.01HCl to 0.1N HCl) for 10min at 37°C, washed with dH_2O (4x, 1 min), and then treated with hyaluronidase (H-3506, Sigma-Aldrich) solution at 1mg/mL (in 0.1M phosphate buffer, pH 5.0) for 30min at 37ºC and washed with dH_2O (4x, 1 min).

(iv) For antigen retrieval for COL VI, hydrated sections were treated with 20 µg/mL proteinase K (EO0491, Thermo Fisher) for 15min at 37ºC.

(v) Blocking buffer constituted of PBS-T containing 2% BSA (ALB-001, albumin-bovine serum fraction V, Bioshop) and 2% horse serum (16050122, GIBCO).

(vi) PBS-T was composed of D-PBS containing 0.05% Tween-20 (TWN510, Bioshop).

Transplantation of *ex vivo*-generated cartilages in rat femoral defects:

Animals care:

Male homozygous athymic nude rats, also known as NIH nude rats (Crl:NIH-*Foxn1*^{rnu}; *rnu*/*rnu*) were purchased from Charles Rivers, USA (1.800.LABRATS). **T**he *rnu*/*rnu* rat is T-cell deficient and shows depleted cell populations in thymus-dependent areas of peripheral lymphoid organs. Animals have been in use for xenograft research to avoid cross-species rejection (Linden and Johansson, 1988). Animal use protocol (AUP) was approved by animal resources center (ARC) of University Health Network (UHN), Toronto, Canada. Upon arrival, rats were allowed to acclimatize for three days to new housing. Animals were provided with sterile housing, food and drinking water.

Surgeries:

Surgeries were conducted on animals at the age of 8-9 weeks and sterile procedures were used at each step. Rats were anesthetized using 5% isoflurane (inhalation anesthetic) and maintained at 2% isoflurane during 20-35min of surgery duration. Pre- and post-operative care was provided to animals. Rats received one injection of analgesia (Buprenorphine, 0.03mg/kg) just before the beginning of surgery and two injections daily (morning and evening) upto three days post-surgery. Animals were kept hydrated by *sc* injections of warm saline (maximum 2 ml per rat) on the back area from the start to the end of surgical procedure. Surgeries were conducted on a clean bench covered with sterile drape sheets cushioned and warmed underneath at 38˚C with a heating pad. Rat knees and surrounding area was shaved and cleaned with iodine surgical scrub (7.5% iodine), 70% isopropanol and 10% Providone iodine (equivalent to 1% iodine) in sequence. A longitudinal incision was made on the anterior aspect of the right knee with a scalpel handle no. 3/blade no. 15 (M90-15, Almedic). The skin, underneath around the knee, was gently dislodged from the subcutaneous layer by using two backward strokes of scissors. A lateral peripatellar incision was made on the subcutaneous layer to expose the outer surface of the knee capsule. The muscle layer lateral and just proximal to knee capsule along with the quadriceps tendon was pushed laterally to expose trochlear region of femur without opening most part of knee capsule. Two chondral defects (≈0.5mm apart, one proximal, one distal) were created in the femoral trochlear groove with the help of a corer (1.45mm, outer diameter, 17guaze, 18035-80, Fine Scientific Tools). The deepening of chondral defect was stopped as soon as mild bleeding was visible in the defect (that ranged from 1.2 mm-1.5mm). There was no attempt to infiltrate the subchondral bone to enter the bone marrow cavity. In some cases, the bottom of the defect was made smooth flat with the help of a beveled needle and the contents were removed by slow suction.

Femoral defects were transplanted with *ex vivo*-generated cartilages with the help of a pasteur pipette and piston (taken from a Hamilton syringe). The diameter of pasteur pipette tip hole was adjusted equal to the diameter of knee defect with the diamond pencil used as a cutter. A round cartilage piece was cut by pushing the sharp end of the glass pasteur pipette over the disc cartilage, and the cartilage plug was dispensed on the top of the rat knee defect with the help of piston. The cartilage piece was pushed in the defect using the piston and than pushing to fit with the help of sterile cotton gauze. The transplanted defect was sealed with 6µl fibril glue (TISSEEL, fibrin sealant, Baxter). The fibrin glue was prepared by mixing equal volume of two components (Sealant and thrombin) right on the transplanted defect. The control defects were transplanted with fibril glue only. The muscle layer along with quadriceps tendon was reverted back to their normal position. The subcutaneous layer was sutured with 5-0 Polysorb™ suture (braided absorbable, UL-202, Covidien) in a discontinuous manner. Skin was closed using intradermal continuous suturing system using Monocryl (Y303, Ethicon) suture. Finally the sutured skin was glued with a thin layer of Vetbond (3M). Animals were placed under warm lamp till they started move freely (generally it took 1-8 min). Animals were allowed to move freely in the cage. Animals were checked twice daily for 3 days, than daily for next 4 days and than twice a week daily till 8 weeks. A total of 28 animals underwent femoral defect surgery in right knee and the defects were immediately transplanted with *ex vivo*-generated cartilage or fibrin glue. The experimental plan is summarized in Table 3.

Tissue retrieval: Animals were euthanized 8 weeks after surgery by using carbon dioxide gas following animal research committee protocol. Right knee was cut from the rest of limbs with the help of a dremel, femur was exposed, and the defects were photographed immediately under a stereomicroscope. The tissues were placed in 10% neutral buffered formalin (HT501128, Sigma-Aldrich) for 3 days with 2 changes. The tissues were removed from formalin, rinsed once with PBS and decalcified for approximately 10 days in Immunocal™ decalcifier solution [1414(DE), DECAL company] with 4 changes. The tissues were processed for paraffin blocks through histological core laboratory and 4µm tissue sections were cut and used for immunohistochemistry for COL II staining and Safranin O staining for proteoglycans staining.

Table 3. Plan for surgical induction of defects in the right knee of athymic nude rat, and, in turn, repair by transplanting with *ex vivo*-generated cartilage at 4 weeks from different groups as indicated.

Group Number of athymic nude rats in each group=7; Number of defects on right knee of each rat=2; Age of rats: 8-9wks	Knee defects of each rat were transplanted with the following:	Rats were sacrificed 8 weeks after transplantations in defects. Right knee was analyzed for integration of transplanted fibrin glue or *ex vivo*-generated cartilage by
Control	Fibrin glue	Collagen II immunohistochemistry, and Safranin O staining on paraffin-embedded sections
MSCs_MO	*Ex vivo*-generated MSCs_MO cartilage at 4 weeks	Same as above
MSCs_FGF2	*Ex vivo*-generated MSCs_FGF2 cartilage at 4 weeks	Same as above
MSCs_FGF2+WNT3A	*Ex vivo*-generated MSCs_FGF2+WNT3A cartilage at 4 weeks	Same as above

RESULTS

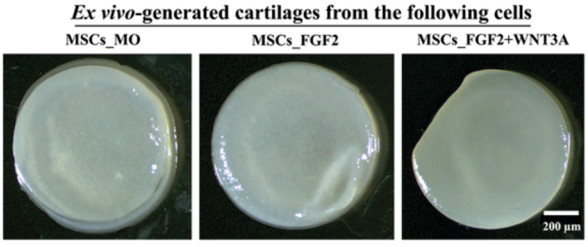

Figure 1. Cartilages generated *ex vivo* at 4 weeks from MSCs expanded in MSCs medium only (MSCs_MO cartilage) or MSCs medium containing FGF2 (MSCs_FGF2 cartilage) or MSCs medium containing FGF2+WNT3A (MSCs_FGF2+WNT3A cartilage) for one passage before chondrogenesis begins.

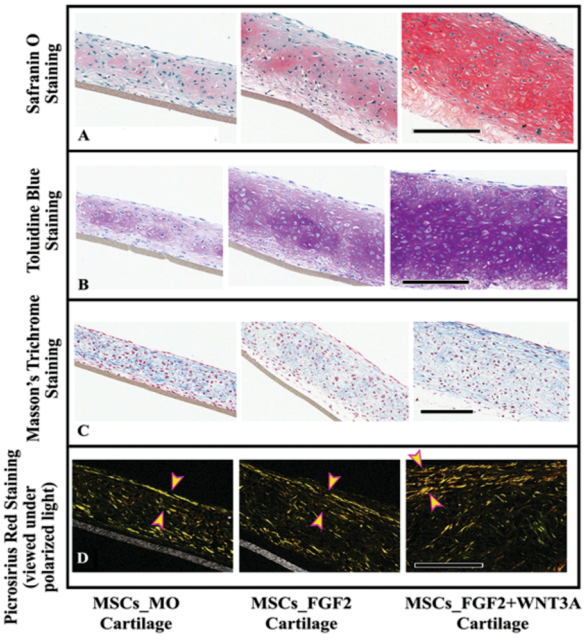

Figure 2. Safranin O (A), Toluidine blue (B), Masson's trichrome (C) and picrosirius red staining (D) of paraffin-embedded sections of *ex vivo*-generated cartilages at 4 weeks from the three groups as indicated. Picrosirius red sections were viewed under polarized light (D). Arrow indicates superficial tangential zone (STZ) of cartilage. Scale bar=300µm.

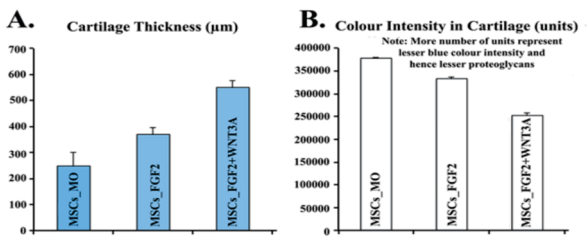

Figure 3. A. Thickness of *ex vivo*-generated cartilages at 4 weeks. Each group differed from each other at P<0.001. B. Measurement of blue colour intensity of Toluidine blue-stained cartilage sections. Each group differed from each other at P<0.001.

Morphology of *ex vivo*-generated cartilages

Ex vivo-generated cartilages from bone marrow-derived MSCs at 4wks from MSCs_MO, MSCs_FGF2, and MSCs_FGF2+WNT3A groups are shown in Figure 1. Cartilage groups differed in hardness. MSCs_FGF2+WNT3A cartilages were harder than MSCs_FGF2 and MSCs_MO cartilage groups, and, in turn, MSCs_FGF2 cartilages were harder than MSCs_MO cartilages. Though we did not do any quantitative measurement to assess hardness of cartilages through mechanical means. The thickness of *ex vivo*-generated cartilages differed among the three groups as described below.

Safranin O, Toluidine blue, Masson's trichrome and picrosirius red staining of paraffin-embedded sections of *ex vivo*-generated cartilages

Figure 2 shows Safranin O (Fig. 2A), Toluidine blue (Fig. 2B), Masson's trichrome (Fig. 2C) and picrosirius red (Fig. 2D) stained sections of *ex vivo*-generated cartilages. Colour intensity of Safranin O staining was higher in MSCs_FGF2+WNT3A cartilage group than MSCs_FGF2 cartilage and MSCs_MO cartilage group. Also the colour intensity was higher in MSCs_FGF2 cartilage group than MSCs_MO cartilage group (Fig. 2A). In Safranin O staining, proteoglycans are assessed in the cartilage (present study, Fig. 2A) and in mucin rich tissues. Safranin O stains proteoglycans orange to red, and nuclei black with background bluish green.

Thickness of *ex vivo*-generated cartilages was measured on Toluidine blue-stained sections (Fig. 2B). MSCs_MO, MSCs_FGF2, MSCs_FGF2+WNT3A cartilage groups had mean thickness of 247±53µm, 369±22µm and 550±26µm (±S.D.) respectively (Fig. 3A). The measurements were done at 10 different points from cartilages from 4 different experiments. Cartilage in MSCs_FGF2+WNT3A and MSCs_FGF2 groups had less variation in thickness, whereas cartilage in MSCs_MO group had more variation in thickness especially at the periphery. MSCs_FGF2+WNT3A cartilage group had higher thickness than MSCs_FGF2 cartilage group (P<0.001) and MSCs_MO cartilage group (P<0.001). Also MSCs_FGF2 cartilage group had higher thickness than MSCs_MO cartilage group (P<0.001). The data was analyzed by one-way ANOVA using Tukey's all pair's comparison.

A hallmark feature of mast cells from all species is their strong metachromatic staining with various cationic dyes, such as Toluidine blue. These properties have been used since the late 19th century to identify mast cells as such. The biochemical background for the characteristic staining properties of mast cells is that their secretory granules contain large amounts of proteoglycans. Toluidine blue stains proteoglycans (Fig. 2B) and mast cells red-purple (metachromatic staining) and the background blue (orthochromatic staining). On Toluidine blue sections, intensity of blue colour of MSCs_ FGF2+ WNT3A cartilage group was significantly higher than MSCs_FGF2 cartilage group (P<0.001) and MSCs_MO cartilage group (P<0.001). Also the blue colour intensity of MSCs_FGF2 cartilage group was higher then that of MSCs_MO cartilage group (P<0.001) (Fig. 3B). The colour intensity was measured using image scope with an algorithm set for black colour as zero and for white color as 255. The measurement of blue coloured sections of Toluidine blue are shown in Figure 3B. More the unit numbers, less the blue colour intensity. The

blue color intensity was 252453±2477 (more dark blue), 333929±3392 (mild dark blue) and 377545±5876 units (light blue) (±S.E.M.) in MSCs_FGF2+WNT3A, MSCs_FGF2, and MSCs_MO cartilage group, respectively (Fig. 3B). The data was analyzed by one-way ANOVA using Tukey's all pair's comparison. The color intensity was measured from 20 randomly chosen spots (area: 507 μm^2) from stained sections from 4 experiments.

All the *ex vivo*-generated cartilage groups showed Masson's trichrome staining that detects collagen, though there was no difference of blue colour intensity between different cartilage groups (Fig. 2C). In this staining assay, the collagen fibers stain blue, the nuclei stain black and the background stain red. Picrosirius red staining is for collagen also. In bright-field microscopy collagen is red on a pale yellow background, and nuclei black or grey or brown (images not included). Picrosirius red stained sections were viewed under polarized light that show the orientation of collagen fibrils (Fig. 2D). According to Junqueira et al. (1979), the birefringence is highly specific for collagen. In the STZ region of all the cartilage sections, the collagen fibrils are parallel to surface, whereas, in other region of cartilage, the collagen fibrils oriented in multiple directions (Fig. 2D). There was no difference of collagen fibrils in the cartilages between different groups (Fig. 2D). Generally, green to greenish yellow represents thin or poorly packed collagen fibrils while yellowish-orange through orange to red represents thick or tightly packed collagen fibers.

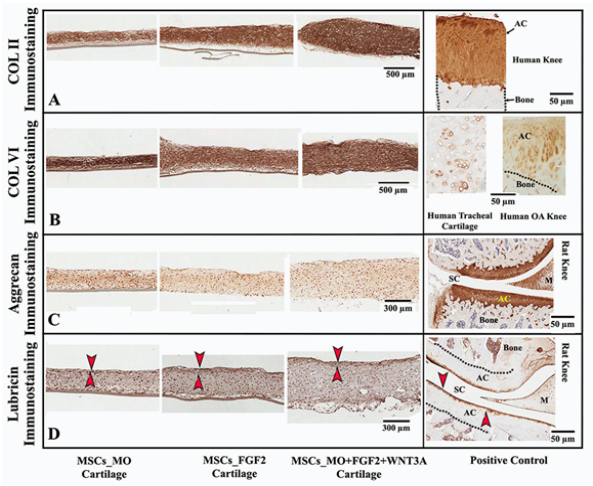

Figure 4. Immunohistochemistry of COL II, COL VI, aggrecan and lubricin on paraffin-embedded sections of *ex vivo*-generated cartilages in different groups as indicated. Human knee served as positive control for COL II in which AC showed positive staining for COL II (A). Human tracheal cartilage served as positive control for COL VI in which chondrocytes show positive staining (B). Also human OA knee served as positive control for COL VI, in which AC showed positive immunostaining (B). Rat knee served as positive control for aggrecan showing immunostaining in AC and also in meniscus (C). Rat knee served as positive control for lubricin in which superficial tangential zone (arrowhead) show positive immunostaining (D). Negative control for each cartilage group did not show positive immunostaining (images not shown). Arrowheads indicate superficial tangential zone of cartilage. AC=articular cartilage; SC=synovial cavity; M=meniscus.

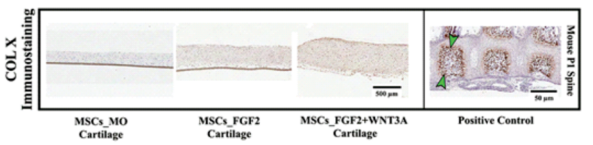

Figure 5. Immunohistochemistry of COL X on paraffin-embedded sections of *ex vivo*-generated cartilages from different groups as indicated. Mouse P1 undecalcified spine served as a positive control. Arrowheads show hypertrophic chondrocytes. Negative control for each cartilage group did not show positive immunostaining for COL X (images not shown).

***Ex vivo*-generated cartilages showed positive staining for COL II, COL VI, aggrecan and lubricin and negative staining for COL X**

Immunohistochemistry of COL II, COL VI, aggrecan and lubricin on paraffin-embedded sections of *ex vivo*-generated cartilages in different groups is shown (Fig. 4A, 4B, 4C, 4D). All the cartilage groups showed positive immunostaining for COL II, there was no difference in the intensity of COL II immunostaining between different cartilage groups (Fig. 4A). Human knee served as positive control indicating positive immunostaining for COL II in articular cartilage (AC) region, and there was no immunostaining in bone region of the knee (Fig. 4A). COL VI immunostaining was present in cartilages from all the groups; the intensity of immunostaining did not differ among different groups (Fig. 4B). Human tracheal cartilage, serving as positive control, showed positive immunostaining for COL VI. Also human OA knee, serving as a positive control, articular cartilage (AC) region showed positive immunostaining for COL VI (Fig. 4B). Aggrecan immunostaining was present in cartilages from all the groups; the intensity of immunostaining did not differ among the groups (Fig. 4C). Rat knee joint, serving as a positive control, showed positive immunostaining for aggrecan in articular cartilage (AC) region and in meniscus region (M) (Fig 4C). Cartilages from all the groups showed immunostaining for lubricin in superficial tangential zone (STZ) with no difference between different groups (Fig. 4D). Rat knee served as positive control for lubricin where STZ region showed positive immunostaining for lubricin (Fig. 4D).

COL X is a marker for hypertrophic chondrocytes. Immunohistochemistry of COL X on paraffin-embedded sections of *ex vivo*-generated cartilages from different groups showed no immunostaining for COL X (Fig. 5). Mouse P1 undecalcified spine served as a positive control that showed hypertrophic chondrocytes in the vertebral bodies showing positive immunostaining for COL X (Fig. 5).

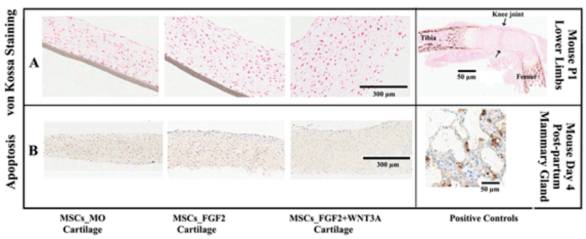

Figure 6. von Kossa staining (A) and apoptosis (B) on paraffin-embedded sections of *ex vivo*-generated cartilages as indicated. Mouse P1 undecalcified lower limbs served as positive control for von Kossa staining in which mineralization is present in lower limbs. Mouse day 4 post-partum mammary gland served as positive control for apoptosis in which regressing secretory cells show apoptosis.

von Kossa staining from all the groups did not show von Kossa positive staining (Fig. 6A). Undecalcified limbs of P1 mouse served as positive control that showed mineralization in the limbs to indicate beginning of osteogenesis in the limbs. In positive von Kossa sections, calcium salts deposits stain brown black, indicating mineralization and the nuclei stained pink. Apoptosis, conducted by tunnel assay (AopTag kit), on *ex vivo*-generated cartilage sections from all the groups, showed no sign of cell death (Fig. 6B). Day 4 post-partum mouse involuted mammary gland, served as positive control that shows apoptosis of mammary secretory cells due to regression.

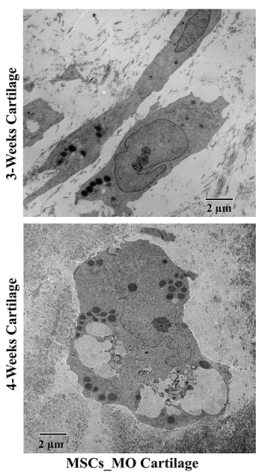

Figure 7. TEM of in *ex vivo*-generated cartilage in MSCs_MO

cartilage group at 3- and 4-weeks. Dark spots show lipid droplets. Note very lobulated shape of nucleus at 3- and 4-weeks cartilage. Assessment of 4-weeks cartilage is summarized in Table 4.

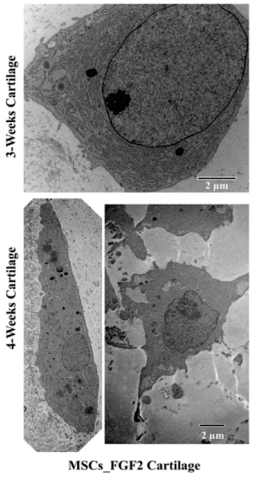

Figure 8. TEM of in *ex vivo*-generated cartilage in MSCs_FGF2 cartilage group at 3- and 4-weeks. Dark spots show lipid droplets that are rare in this group. Note more oval shaped nucleus and less indented nuclei in this group at 3-and 4-weeks cartilages. Assessment of 4-weeks cartilage is summarized in Table 4.

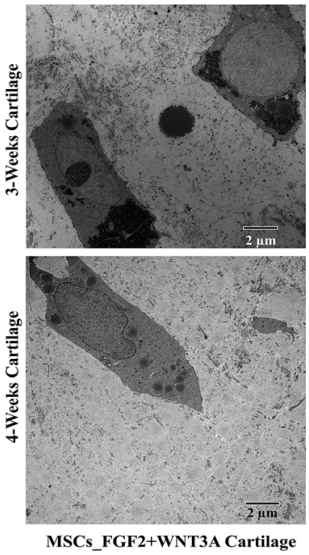

Figure 9. TEM of in *ex vivo*-generated cartilage in MSCs_FGF2+ WNT3 A group at 3- and 4-weeks. Dark spots show lipid droplets. Note more oval shaped nucleus in 3-weeks cartilage and some lobulated nucleus shape in 4 weeks cartilage. Assessment of 4-weeks cartilage is summarized in Table 4.

Table 4. Comparison of assessment of TEM images from all the three groups of *ex vivo*- generated cartilages. Number of TEM images assessed=20 in each cartilage group in one experiment. Number of experiments=3.

MSCs_MO Cartilage	MSC_FGF2 Cartilage	MSC_FGF2+WNT3A Cartilage
Cells are flattened or rounded with an irregular surface (stellate shaped) but most cells appeared rounded and **hypertrophied.**	Cells are flattened or rounded but in both cases with an irregular surface (stellate) but most cells appeared flattened.	Flattened and rounded cells but cells are mostly rounded with an irregular surface (stellate).
Nucleus is sizeable, rounded generally indented and lobulated in many instances. Nucleus generally with euchromatin.	**Nucleus ovoid generally** with heterochromatin	**Nucleus rounded and partly lobulated in many cases** generally with euchromatin
Nucleolus present	Nucleolus present	One or more nucleoli present
rER (++)	rER (+)	rER (++++)
		glycogen (++)
Lipid droplets (+++) Some lipid droplets found in the midst of large secretory vacuoles	**Lipid droplets (scarce)**	**Lipid droplets (++)**
Large secretory vacuoles (+++)	Large and small secretory vacuoles (++++) of light density.	Large and small secretory vacuoles (+++) of density similar to the ECM
	Dense bodies (++)	Dense bodies (+)
ECM (++++)	ECM (+)	ECM (+)
No periodicity in the collagen fibers.	No periodicity in the collagen fibers.	No periodicity in the collagen fibers.

Transmission electron microscopy (TEM) of *ex vivo*-generated cartilages

Representative TEM images of *ex vivo*-generated cartilages at 4-weeks, for all the groups, are shown (Fig. 7, 8, 9). Additionally, we have added 3-weeks cartilage images also in these Figures for extra information. Professor Dr. R Marc Pelletier (University de Montreal, Canada) assessed week-4 TEM images, and the report is summarized in Table 4. TEM of *ex vivo*-generated cartilages indicated that MSCs_FGF2 cartilage group has chondrocytes with more ovalness and with rarely seen lipid droplet. The nucleus shape was best (more oval) in MSC_FGF2 cartilage group and worst in MSCs_MO (lobulated and indented) cartilage group. The number of lipid droplets was higher in MSCs_MO cartilage group than MSCs_FGF2+WNT3A group, which, in turn, was higher than that of MSCs_FGF2 group (Table 4). More hypertrophied shaped cells were found in MSCs_MO cartilage group.

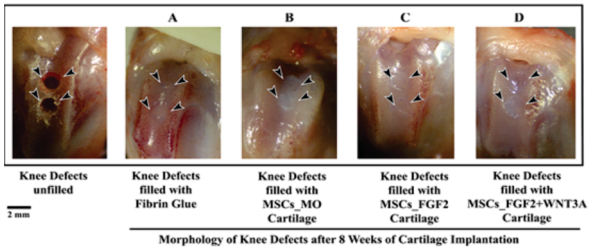

Figure 10. Morphology of whole mounts of athymic nude rat knee exhibiting defects. Left panel shows the un-transplanted knee defect and right panels exhibit transplanted knee defects (Fig. A, B, C, D; arrow points to the defect). Apparently, knee defects transplanted with either fibrin glue (A) or with *ex vivo*-generated MSCs_MO cartilage (B) or MSCs_FGF2 cartilage (C) or MSCs_FGF2+WNT3A cartilage (D) look morphologically similar.

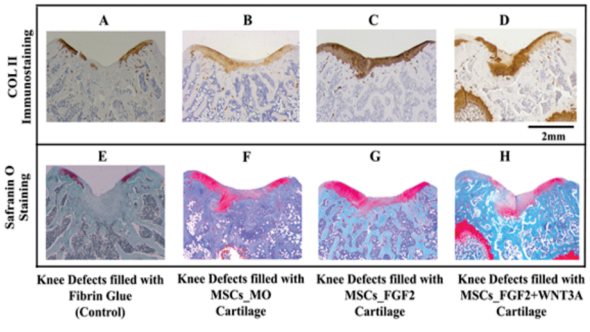

Figure 11. Histological assessment of athymic nude rat knee defects after 8 weeks of transplantation. A-D. COL II immunohistochemistry of paraffin-embedded sections of the transplanted defects from different groups as indicated. E-H. Safranin O staining of paraffin-embedded sections of the transplanted defects from different groups as indicated.

Assessment of knee defects transplanted surgically with fibrin glue or *ex vivo*-generated cartilages

There was no immunostaining for COL II (Fig. 11A) and Safranin O staining (Fig. 11E) in the defects transplanted with fibrin glue only, respectively. Thus transplantation of defects showed fibrous tissue only with no cartilaginous extracellular matrix (Figures 11A, 11E). Transplantation of knee defects were positive for COL II immunostaining for the defects transplanted with *ex-vivo* generated cartilage from different groups as indicated (Fig. 11B, 11C, 11D). Transplantation of knee defects were also positive for Safranin O staining for the defects transplanted with *ex-vivo* generated cartilage from different groups as indicated (Fig. 11F, 11G, 11H). After comparing and scoring the knee defects transplantations between different cartilage groups, it was found that knee defects transplanted with MSCs_FGF2 cartilage scored best (Fig. 11C, 11G), and defects transplanted with MSCs_FGF2+WNT3A cartilages scored second best (Fig. 11D, 11H) and defects transplanted with MSCs_MO cartilages scored least (Fig. 11B, 11F) successful. A total of 56 defects were assessed from 28 rats, 14 defects were transplanted with fibrin glue only and 14 were transplanted with cartilage from each group. Two independent observers conducted scoring.

DISCUSSION

In this investigation, we used animal model to treat injury-induced chondral knee defects. We generated cartilages *ex vivo* that were disc-shaped, and were generated from bone marrow-derived MSCs. Bone marrow was aspirated from patients undergoing TKR or THR procedures.

Cartilages were generated on collagen-coated inserts in the wells of 24-well plates. In our earlier study, we generated micromass cartilages from human bone marrow using some of the similar procedures (Juneja *et al*., 2016) as described here. In the current study, we added additional steps by expanding MSCs in the presence of either in 'MSCs medium' or in MSCs medium containing FGF2 or in MSCs medium containing FGF2 +WNT3A for one passage before chondrogenesis. Furthermore, we transplanted *ex vivo*-generated cartilages in the chondral knee defects of athymic nude rats created surgically, and assessed their role to treat injury-induced knee defects after 8 weeks simulating treating human OA defects. The purpose of using athymic nude rats in this study was to avoid rejection of human tissue from athymic nude rats.

There are multiple reports available for the use of MSCs and or chondrocytes for the repair of cartilage defects in animal models or human. Ebihara and group used layered chondrocyte sheets to repair cartilage full thickness defects in mini-pig model. Good Safranin-O staining, and integration with surrounding tissues was achieved in animals transplanted with layered chondrocyte sheets. However, tissue had poor Safranin-O staining in the domestic rabbit experiment and also the subchondral bone was poorly repaired (Ebihara *et al*., 2012). Prasadam and team mixed bone marrow-derived MSCs (BMSCs) and articular cartilage chondrocytes (ACCs) in a 1:1 ratio and tested for their ability to enhance cartilage regeneration in an intra-articular injection in a meniscectomy-induced osteoarthritis rat model. They noticed significantly enhanced cartilage regeneration and decreased fibrosis in the mixed BMSCs+ACCs group as compared with the monocultures. Molecular analysis also showed a reduction in hypertrophy with higher chondrogenic gene expression (Prasadam *et al*., 2018). Jia's group made cartilage defects in the patellar grooves of New Zealand white rabbits. The rabbit synovial fluid-derived MSCs were generated from the knee cavity by arthrocentesis. Hyaline-like cartilage was detected in the defects treated with these MSCs, while fibrocartilage tissue formed in the defects treated with chondrocytes derived from these MSCs (Jia *et al*., 2018). In another study, allogeneic MSCs mixed with either 10% or 20% recycled autologous cartilage-derived cells (chondrons) for treatment of cartilage defects in the knee in symptomatic cartilage defect patients. This unique study in man demonstrated no treatment-related adverse events up to one year postoperatively. At 12 months, all patients showed statistically significant improvement in clinical outcome compared to baseline (de Windt *et al.,* 2017). Ha and group reviewed the role of intra-articular MSCs in OA of the human knee (Ha et al., 2019). Intraarticular MSCs provide improvements in pain and function in knee osteoarthritis at short-term follow-up (<28 months) in many cases. Some efficacy has been shown of MSCs for cartilage repair in osteoarthritis; however, the evidence of efficacy of intra-articular MSCs on both clinical outcomes and cartilage repair remains limited. In an unpublished experiment, we did inject 3 million MSCs in MMx (medial meniscectomized)-induced OA athymic nude rat knee capsule but unfortunately there was no repair of MMx-induced OA in athymic nude rat at 10 weeks post-treatment, rather they did harm the knee cartilage as evidenced by histology (unpublished, Juneja, S.C.). However, in the current study, we transplanted *ex vivo*-generated cartilages derived from MSCs expanded for one passage with growth factors (FGF2 or FGF2 and WNT3A) in the knee defects of athymic nude rat and the assessment of knee defects was made at 8 weeks post-surgery.

ten Berge and coworkers showed that Wnt and FGF signals interact to coordinate growth and cell fate specification during limb development. In the newly established limb bud (E9.5) in mouse, both Wnt and FGF proteins signal throughout the limb mesenchyme and maintain all cells in a multi-potent, proliferative state (ten Berge *et al*., 2008). Following limb outgrowth, cells in the center of the limb are no longer within range of the signals. This allows cell cycle withdrawal and expression of Sox9, leading to establishment of the chondrogenic core. Coordinated role of WNT and FGF encouraged us to use FGF and WNT for MSCs expansion before chondrogenesis begins. Based on developmental mechanism, we planned the exposure of FGF and WNT during MSCs expansion before placing in CCM simulating the developmental mechanism (Table 3).

MSCs_FGF2+WNT3A cartilages were thicker and had more proteoglycans, in the current studies (Fig. 2, 3). FGF-2 may influence two aspects of MSCs chondrogenesis. First, the growth factor may speed the sequential, time-dependent pattern of gene expression that occurs during cartilaginous differentiation (Barry *et al*., 2001; Mwale *et al*., 2006), leading to earlier production of cartilage-associated molecules. FGF-2 treatment may lead to an altered phenotypic in cartilage that resembles native cartilage. Current methods for MSCs chondrogenesis lead to tissues that do not match the biochemical and biomechanical properties of native cartilage (Mauck *et al*., 2006; Huang *et al*., 2010). Bioactive molecules can influence both kinetics and phenotype during differentiation. For instance, TGF-β strongly influences MSCs phenotype, leading to chondrogenesis rather than other programs of differentiation. Growth factors can also affect the kinetics of differentiation. For example, BMP-6 accelerates the differentiation of limb-bud mesenchymal cells into hypertrophic chondrocytes *in vitro* (Boskey *et al*., 2002). The current study used TGFβ3 (10ng/ml) as chondrogenic factor in complete chondrogenesis medium as described earlier (Juneja *et al*., 2016). And we used FGF2 and WNT3A supplements in MSCs expansion medium for one passage before chondrogenesis.

It is unclear whether FGF-2 affects MSCs phenotype, the kinetics of MSC differentiation, or both factors. Most previous studies have evaluated differentiation at single time points without addressing temporal changes. The studies that have assessed multiple time points have shown large differences in gene expression and GAGs content early, but have suggested that differences may diminish later (Solchaga *et al*., 2005, 2010). In the current investigation, MSCs expanded for one passage before chondrogenesis in MSCs medium supplemented with FGF2 (*i.e.,* MSCs_FGF2) or with FGF2+WNT3A (*i.e*., MSCs_FGF2+WNT3A) had higher proteoglycan-rich matrix and higher cartilage thickness than MSCs expanded in medium alone (*i.e*., MSCs_MO) at 4 weeks of chondrogenesis (Figures 2A, 2B, 3A, 3B). That was shown by higher Safranin O staining and higher intensity of blue colour by Toluidine blue staining in MSCs_FGF2 and MSCs_FGF2+WNT3A cartilage groups as compared to MSCs_MO) cartilage group. Also MSCs_FGF2+WNT3A cartilage group has additional extra blue colour intensity and thickness over MSCs_FGF2 cartilage group.

Safranin O is a metachromatic cationic dye and stains Gram-negative bacteria pink to red. It is also used to assess proteoglycans in cartilage. The dye imparts an intense red to GAGs of proteoglycans. Safranin O has been used to stain matrix proteoglycans to study cartilaginous tissue structural integrity in mice (Almonte-Becerril *et al*., 2018). It has also been used to stain differentiated tissues through chondrogenesis from human bone marrow MSCs (Suzuki *et al*., 2012), *ex vivo*-generated pellet cartilage (Bae *et al*., 2018) and iPSCs-derived cartilage tissues (Diekman *et al*., 2012; Gardner *et al*., 2019). Use of Toluidine blue in tissue sections is done with the aim to highlight cartilage (Sridharan *et al*., 2012). Selective binding of Toluidine blue to basophilic proteoglycans is the first stage of a staining method that proceeds to the formation of a heavy metal salt of the dyestuff. By means of this procedure, matrix complexes of hyaline cartilage were stained (Sridharan *et al*., 2012). The findings are interpreted as the

demonstration of proteoglycan constituents of chondromucin aggregates. Toluidine blue staining method has been used to localize proteoglycans by many investigators in *ex vivo* including micromass or pellet chondrogenesis cultures (Suzuki *et al*., 2012; Peran *et al*., 2013). Wei and team compared Toluidine blue staining on cartilage sections from OA and normal subjects. OA cartilage has much lower Toluidine blue staining indicating loss of proteoglycans due to OA (Wei *et al*., 2012).

Total collagen was assessed in micromass cultures derived from hESCs by Masson's trichrome staining (Toh *et al*., 2009). Peck and team questioned and verified stains for collagen that existed but it was unclear to them whether the stains bind stoichiometrically to collagens (Peck *et al*., 2015). The aim of their study was to clarify whether traditional collagen stains*, i.e.,* Masson's trichrome or picrosirius red, could be used for quantification of the collagen content in articular cartilage. Based on their findings, picrosirius red and modified Masson's trichrome were more suitable for quantification of articular cartilage collagen content than standard Masson's trichrome. In our study, we used traditional Masson's trichrome staining method; all the cartilage groups showed the presence of collagen but there was no difference between the cartilage groups (Fig. 2C). We also used picrosirius successfully to localize collagen fibers in the cartilages from all the groups (Fig. 2D). Hindle and team were able to use Masson's trichrome staining method to assess collagen in repaired defects in articular cartilage in sheep knee with autologous MSCs using hydrogels and collagen membranes (Hindle *et al*., 2016). In a pellet culture, birefringent collagen fibers show developing zonation in the newly formed hyaline matrix and parallel to the pellet surface horizontal arranged birefringent fibers in the margin. Randomly organized collagen fibers were found in the central area. Perpendicularly oriented birefringent fibers were located in proximity to the cell-condensed center (Walzer *et al*., 2019). In our cartilage system, the collagen fibers in STZ layer were parallel to the cartilage surface (Fig 2D). Truong and team used picrosirius red staining method to detect total collagen in repaired full thickness knee defects after 12 weeks (Truong *et al.,* 2017).

Immunostaining of paraffin sections of *ex vivo*-generated cartilages at 4 weeks with specific antibodies to COL II, COL VI and aggrecan demonstrated that chondrocytes with abundant cartilage specific matrices existed in the disc cartilages (Figs. 4A, 4B, 4C). The immunostaining of lubricin in STZ region of disc cartilage further proved this tissue to be of articular cartilage nature simulating the articular cartilage in control cartilage (Fig 4D). The absence of COL X indicated that there were not any hypertrophic chondrocytes of osteogenesis nature in our *ex vivo* generated cartilages. Similar antigens have been reported to be present in differentiated cells or tissues derived after MSCs chondrogenesis using immunohisto chemistry or gene expression by RTPCR procedures (Mwale *et al*., 2006; Twomey *et al*., 2014 Nakagawa *et al*., 2016; Yang *et al*., 2018)

von Kossa staining of paraffin-embedded sections of *ex vivo*-generated cartilage from all the groups exhibited negative staining. The assay demonstrated that there was no osteogenesis in our cartilage assay (Fig. 6A) as compared to positive control in which postnatal day 1 mouse undecalcified long bones showed mineralization in the bones (Fig. 6A). Using this assay, Chijimatsu and coworkers assessed the osteogenic differentiation of MSCs-like cells, and found positive staining during MSCs osteogenesis differentiation (Chijimatsu *et al*., 2017). On 8th day of osteogenesis differentiation of MSCs, mineralization was found positive using von Kossa staining (Kruger *et al*., 2012).

Apoptosis assay of *ex vivo*-generated cartilage from all the groups showed no sign of cell death (Fig. 6B). Involuted day-4 post-partum mouse mammary gland, served as positive control. That showed apoptosis of milk secreting cells of mammary gland due to regression (Fig. 6B). Absence of apoptosis in our *ex vivo*-generated cartilages indicated the good quality of our culture system. Wang and coworkers studied culture conditions affecting apoptosis during chondrogenesis from MSCs as determined by Annexin V, TUNEL staining and lysosomal labeling during chondrogenesis. The authors claimed that MSCs undergoing chondrogenesis are associated with multiple apoptosis pathways and those may be inhibited by TGFβ1. TGFβ1also increased the expression/synthesis of chondrogenic matrices and decreased the expression of osteogenic genes (Wang *et al*., 2010). We used TGFβ3 in complete chondrogenesis medium (CCM) and found no apoptosis in chondrocytes in *ex vivo*-generated cartilages from all the groups at 4 weeks of chondrogenesis. Chondrogenic markers expressed well in our system as shown by immunohistochemistry in all the three groups of cartilages, and also there was absence of osteogenic gene (Fig 4, 5). We studied apoptosis by tunnel assay and used involuted day-4 post-partum mammary gland as a positive control, which is a good marker for apoptosis (Fig. 6B). During involution of mammary gland, when pups are removed from mother, mammary gland starts to regress and that causes apoptosis of milk secretory cells and hence is a good marker for apoptosis positive control. MSCs chondrogenesis differentiation *in vitro* did not show apoptosis in micromass and pellet cultures (Ichinose *et al*., 2010). Tallheden and coworkers reported that chondrocytes did not express apoptosis-related genes during *in vitro* chondrogenesis (Tallheden *et al*., 2004).

TEM of 3-weeks and 4-weeks cartilages from all the group showed that shape of the nucleus of chondrocytes was more oval in MSCs_FGF2 group and with lowest number of lipid droplets among all the groups. In MSCs_MO cartilage group, maximum number of lipid droplets existed among all the groups (Fig. 7, 8, 9). The shape of the nucleus in chondrocytes was more abnormal with indentation and or lobulation as compared to other two groups.

MSCs_FGF2+WNT3A cartilage group showed the nucleus feature and lipid droplets feature in between MSCs_MO and MSCs_FGF2 groups. MSCs_FGF2+WNT3A had some lipid droplets, that were more than MSCs_FGF2 but less than MSCs_MO cartilage groups. The shape of nucleus was partially lobulated or with minor indentation. MSCs_FGF2 cartilages graft transplanted best in rat knee defects among all the three groups. The information clearly may relate, the lesser the lipid droplets and better the oval shaped nucleus better the chance of transplantation. The nucleus shape and number of lipid droplets in chondrocytes may relate to the development of osteoarthritis or poor quality of articular cartilage.

TEM study of normal articular cartilage showed scarce lipid droplets (Roy and Meachim, 1968). In an interesting study conducted by PGI Chandigarh and Christian Medical College Ludhiana groups, chondrocyte has more lobulated nucleus and more lipid droplets in aged and OA human knee articular cartilage as compared to that normal knee cartilage (Goyal *et al*., 2013). We showed that *ex vivo*-generated cartilages had chondrocytes with lobulated nuclei and with more lipid droplets in MSCs_MO cartilage group than other two groups and also had poor cartilage transplantation in rat knee and had lower COL II immunostaining and Safranin O staining in the repaired defect (Fig. 11B vs. Fig. 11C and 11D). It clearly shows that the repaired knee defects in MSCs_MO cartilage group synthesized less COL II and exhibited less proteoglycans in knee defects (Fig. 11B, 11F) as compared to other two groups (Fig. 11C, 11G and 11D, 11H).

The defects transplanted with fibrin glue show fibrous tissue and no tissue rich in cartilaginous matrix (Fig. 11A, 11E) and as we reported earlier in rat knee defects (Gardner *et al.,* 2019). The study from Goyal and coworkers supports our lower score of our cartilage transplantation in MSCs_MO group in that chondrocyte has more lipid droplets and chondrocyte nucleus more indented and lobulated.

Auw Yang and coworkers were able to improve the quality of pellet culture after chondrocytes expanded in the presence of FGF2 as compared to cells not exposed to FGF2 during expansion (Auw Yang *et al*. 2006). After 28 days, chondrocyte expansion in bFGF and re-differentiation on collagen-coated filters resulted in better chondrogenesis than chondrocytes expanded in basic expansion medium without bFGF. TEM showed a large number of lipid vacuoles similar to in chondrocytes of *ex vivo*-generated cartilages at 4 week after expanding MSCs culture without FGF2 (Auw Yang *et al*. 2006). Nucleus shape and size can be affected *in vitro* culture conditions depending upon low density or high-density chondrocyte in bead cartilage and their characteristics also depended upon periphery or central chondrocytes in the bead cartilage (Kobayashi, 2013). To avoid this issue, we generated disc cartilage culture where cartilaginous matrices and chondrocytes are supposed to be homogeneous throughout the disc.

SUMMARY AND CONCLUSION

Summary: *Ex vivo*-generated cartilages differed in their properties. Hardness of cartilage was in this order in cartilage groups: MSCs_FGF2+WNT3A > MSCs_FGF2 > MSCs_MO. Thickness of

cartilage was in this order: MSCs_FGF2+WNT3A > MSCs_FGF2 > MSCs_MO (P<0.001).

Proteoglycans in cartilage were in this order: MSCs_FGF2+WNT3A> MSCs_FGF2 > MSCs_MO as determined by toluidine blue staining (P<0.001) as well as by Safranin O staining. All the groups of cartilages showed the presence of positive chondrogenic markers (COL II, COL VI, aggrecan and lubricin) and absence of hypertrophic chondrocyte marker (COL X) as shown by immunohistochemistry. There was no mineralization and apoptosis in cartilages as shown by von Kossa and apoptosis tunnel assay, respectively. TEM showed that chondrocytes in cartilages were from 'best to worst' in this order: MSCs_FGF2 > MSCs_FGF2+WNT3A > MSCs_MO. Chondrocyte quality was assessed by the presence of number of lipid droplets and ovalness of the chondrocyte's nucleus. More the number of lipid droplets in chondrocyte, worst the quality of chondrocyte. More the indented and lobulated nucleus in chondrocyte, worst the chondrocyte. More oval chondrocyte was considered as best chondrocyte. The transplantation success of cartilages was in order from 'best to worst': MSCs_FGF2 > MSCs_FGF2+WNT3A > MSCs_MO groups. Cartilage transplantation success was based on COL II staining and Safranin O staining of defects region.

CONCLUSION:

Ex vivo-generated cartilage, differentiated from MSCs derived from human bone marrow, was able to repair induced-chondral defects in athymic nude rat knee. Using this method, human osteoarthritis can be treated using patient's own bone marrow derived MSCs.

Limitations of the study:

The recovery of rats after cartilage transplantation was at one time point only that was at 8 weeks. Based on good results at 8 weeks study, studies for long-term periods are encouraged in future. Though, we developed a simple method for treatment of OA. But how this procedure will be applied in human knee that will be next challenge. Still we will need to collaborate with bioengineers who have medical background who can come up with less invasive methods which take the damaged pieces out of OA knee capsule and place the good cartilage tissue at the same place without further damaging the knee capsule and causing any technical inflammation or leading to rheumatoid arthritis as side effects.

Conflict of interest: None.

Acknowledgements:

The research was funded by Arthritis Program, Krembil Research Institute, University Health Network (UHN), Toronto, Canada. My thanks are due to Matthew Scaife (UHN), for his advice on MSCs culture; Daniel Antflek (UHN), Amanda Weston (UHN), and Luis Montoya (UHN) for their help on ethics procedure, patient consent and or patient coordination; Milan Ganguly (STTARR facility, UHN, Toronto, Canada) for histological sectioning; Bernard Castro (Sickkids Hospital, Toronto, Canada) for histology sectioning; Heather Whetstone (Sickkids Hospital, Toronto, Canada), Dr. Keenan Thomas (Baylor College of Medicine, Huston), Dr. Matthew Hilton (Duke University, USA) and Dr. Bradley Estes (Duke University, USA) for their suggestions on immunohistochemistry; Howard Rosenberg for processing tissues and making TEM blocks, Tulip and Euman for help in taking TEM images (Sickkids Hospital, Toronto), Professor Dr. Marc Pelletier for reading TEM images (Université de Montreal, Montréal QC, Canada), and Dr. Nizar Mohamed, Dr. Rajiv Gandhi and Dr. Rod Davey (Toronto Western Hospital, Toronto) for bone marrow aspirations from patients.

REFERENCES

1. Almonte-Becerril M, Gimeno-LLuch I, Villarroya O, Benito-Jardón M, Kouri JB, Costell M. 2018. Genetic abrogation of the fibronectin-α5β1 integrin interaction in articular cartilage aggravates osteoarthritis in mice. PLoS One 13: e0198559. PMID: 29870552
2. Alshami AM. 2014. Knee osteoarthritis related pain: a narrative review of diagnosis and treatment. International Journal Health Sciences. 85-104. PMID: 24899883
3. Auw Yang KG, Saris DBF, Geuze RE, van der Helm YJM, van Rijen MHP, Verbout AJ, Dhert WJA, Creemers LB. 2006. Impact of expansion and redifferentiation conditions on chondrogenic capacity of cultured chondrocytes. Tissue Engineering 12: 2435-2447 PMID: 16995777
4. Bae HC, Park HJ, Wang SY, Yang HR, Lee MC, Han HS. 2018. Hypoxic condition enhances chondrogenesis in synovium-derived mesenchymal stem cells. Biomater Res 22: 28. PMID: 30275971
5. Barry F, Boynton RE, Liu B. 2001. Chondrogenic differentiation of mesenchymal stem cells from bone marrow: differentiation-dependent gene expression of matrix components. Exp Cell Res 268: 189-200. PMID: 11478845
6. Boskey AL, Paschalis EP, Binderman I. Doty SB. 2002. BMP-6 accelerates both chondrogenesis and mineral maturation in differentiating chick limb-bud mesenchymal cell cultures. J Cell Biochem 84: 509-519. PMID: 11813256
7. Chijimatsu R, Ikeya M, Yasui Y, Ikeda Y, Ebina K, Moriguchi Y, Shimomura K, Hart DA, Yoshikawa H, Nakamura N. 2017. Characterization of mesenchymal stem cell-like cells derived from human iPSCs via neural crest development and their application for osteochondral repair. Stem Cells International 2017: 1960965. PMID: 28607560
8. Chu CR, Szczodry M, Bruno S. 2010. Animal models for cartilage regeneration and repair. Tissue Engineering Part B: Reviews 16: 105-115. PMID: 19831641
9. de Windt TS, Vonk LA , Slaper-Cortenbach ICM , van den Broek MPH , Nizak R , van Rijen MHP, Weger RA , Dhert WJA , Saris DBF. 2017. Allogeneic mesenchymal stem cells stimulate cartilage regeneration and are safe for single-stage cartilage repair in humans upon mixture with recycled autologous chondrons. Stem Cells 35: 256-264 PMID: 27507787
10. Diekman BO, Christoforou N, Willard VP, Sun H, Sanchez-Adams J, Leong KW, Guilak F. 2012. Cartilage tissue engineering using differentiated and purified induced pluripotent stem cells Proc Natl Acad Sci U S A 109: 19172-19177. PMID: 23115336
11. Ebihara G , Sato M, Yamato M, Mitani G, Kutsuna T, Nagai T, Ito S, Ukai T, Kobayashi M, Kokubo M, Okano T, Mochida J. 2012. Cartilage repair in transplanted scaffold-free chondrocyte sheets using a minipig model. Biomaterials 33: 3846-3851. PMID: 22369960
12. Gardner OF, Juneja SC, Whetstone H, Nartiss Y, Sieker JT, Veillette C, Keller GM, Craft AM. 2019. Effective repair of articular cartilage using human pluripotent stem cell-derived tissue. eCells and Materials Journal 38: 215-227. PMID: 31688947
13. Goyal N, Gupta M, Joshi K. 2013. Ultrastructure of chondrocytes in osteoarthritic femoral articular cartilage. Kathmandu Univ Med J (KUMJ) 11: 221-225 PMID: 24442170
14. Ha CW, Park YB, Kim SH, Lee HJ. 2019. Intra-articular mesenchymal stem cells in osteoarthritis of the Knee: A systematic review of clinical outcomes and evidence of cartilage repair arthroscopy: The Journal of Arthroscopic and Related Surgery. 35: 277-288. PMID: 30455086
15. Hindle P, Baily J, Khan N, Biant LC, Simpson AHR, Peault B. 2016. Perivascular mesenchymal stem cells in sheep: Characterization and autologous transplantation in a model of articular cartilage repair. Stem Cells Dev 25: 1659-1669 PMID: 27554322
16. Huang AH, Stein A, Mauck RL. 2010. Evaluation of the complex transcriptional topography of
17. mesenchymal stem cell chondrogenesis for cartilage tissue engineering. Tissue Eng Part A 16: 2699-2708. PMID: 20367254
18. Ichinose S, Muneta T, Koga H, Segawa Y, Tagami M, Tsuji K, Sekiya I (2010). Morphological differences during in vitro chondrogenesis of bone marrow-, synovium-MSCs, and chondrocytes. Laboratory Investigation. 90: 210-221 PMID: 20010853
19. Jia Z, Liu Q, Liang Y, Li X, Xu X, Ouyang, K, Xiong J, Wang D, Duan L, 2018. Repair of articular cartilage defects with intra-articular injection of autologous rabbit synovial fluid-derived mesenchymal stem sells. J Transl Med 16:123. PMID: 29739472
20. Juneja SC, Viswanathan S, Ganguly M, Veillette C. 2016. A simplified method for the aspiration of bone marrow from patients undergoing hip and knee joint replacement for isolating mesenchymal stem cells and in vitro chondrogenesis. Bone Marrow Research 2016: 3152065. PMID: 27057356
21. Junqueira LC, Bignolas G, Brentani RR. 1979. Picrosirius staining plus polarization microscopy, a specific method for collagen detection in tissue sections, Histochem J 11: 447-455. PMID: 91593
22. Kobayashi S. 2013. Importance of extracellualr environment for regenerative medicine and tissue engineering of cartilagious tissue. Chapter 22. http://dx.doi.org/10.5772/55566. © 2013 Kobayashi; licensee InTech.
23. Kruger JP, Endres M, Neumann K, Stuhlmuller B, Morawietz L, Häupl T, Kaps C. 2012. Chondrogenic differentiation of human subchondral progenitor cells is affected by synovial fluid from donors with osteoarthritis or rheumatoid arthritis. Journal of Orthopaedic Surgery and Research 7:10 PMID: 22414301
24. Lawrence RC, Felson DT, Helmick CG, Arnold LM, Choi H, Deyo RA, Gabriel S, Rosemarie H, Hochberg MC, Hunder GG, Jordan JM, Katz JN, Kremers HM, Wolfe F, National Arthritis Data Workgroup. 2008. Estimates of the prevalence of arthritis and other rheumatic conditions in the United States. Part II. Arthritis & Rheumatology. 58L: 26-35. PMID: 18163497
25. Linden CJ, Johansson L. 1988. Growth of a human pleural mesothelioma xenografted to athymic rats and mice. Br J Cancer 58: 614-618. PMID: 3219271
26. Mak J, Jablonski CL, Leonard CA, Dunn JF, Raharjo E, Matyas JR, Biernaskie J, Krawetz RJ. 2016. Injection of synovial mesenchymal stem cells improves cartilage repair in a mouse injury model. Sci Rep 6: 23076. PMID: 26983696
27. Makris EA, Gomoll AH, Malizos KN, Hu JC, Athanasiou KA. 2015. Repair and tissue engineering techniques for articular cartilage. Nature Reviews Rheumatology. 11: 21-34. PMID: 25247412
28. Mauck RL, Yuan X, Tuan RS. 2006. Chondrogenic differentiation and functional maturation of bovine mesenchymal stem cells in long-term agarose culture. Osteoarthritis Cartilage 14: 179-189. PMID: 16257243
29. Mwale F, Stachura D, Roughley P, Antoniou J. 2006. Limitations of using aggrecan and type X collagen as markers of chondrogenesis in mesenchymal stem cell differentiation. J Orthop Res 24: 1791-1798. PMID: 16779832
30. Nakagawa Y, Muneta T, Otabe K, Ozeki N, Mizuno M, Udo M, Saito R, Yanagisawa K, Ichinose S, Koga H, Tsuji K, Sekiya I. 2016. Cartilage derived from bone marrow mesenchymal stem cells expresses lubricin in vitro and in vivo. PLoS One 11: e0148777. PMID: 26867127
31. Peck Y, He P, Chilla GSVN, Poh CL, Wang DA. 2015. A preclinical evaluation of an autologous living hyaline-like cartilaginous graft for articular cartilage repair: A pilot study. Sci Rep 5: 16225. PMID: 26549401
32. Peran M, Ruiz S, Kwiatkowski W, Marchal JA, Yang SL, Aranega A, Choe S, Belmonte JCI. 2013. Activin/BMP2 chimeric ligands direct adipose-derived stem cells to chondrogenic differentiation. Stem Cell Res 10: 464-476. PMID: 23500646
33. Prasadam I, Akuien A, Friis TE, Fang W, Mao X, Crawford RW, Xiao Y. 2018. Mixed cell therapy of bone marrow-derived mesenchymal stem Cells and Articular Cartilage Chondrocytes Ameliorates Osteoarthritis Development. Lab Invest 98: 106-116. PMID: 29035380
34. Roy S, Meachim G. 1968. Chondrocyte ultrastructure in adult human articular cartilage. Ann rheum Dis 27: 544-558. PMID: 5728099
35. Solchaga LA, Penick K, Goldberg VM, Caplan AI, Welter JF. 2010. Fibroblast growth factor-2 enhances proliferation and delays loss of chondrogenic potential in human adult bone-marrow-derived mesenchymal stem cells. Tissue Eng Part A 16: 1009-1019. PMID: 19842915
36. Solchaga LA, Penick K, Porter JD, Goldberg VM, Caplan AI, Welter JF. 2005. FGF-2 enhances the mitotic and chondrogenic potentials of human adult bone marrow-derived mesenchymal stem cells. J Cell Physiol 203: 398-409 PMID: 15521064
37. Sridharan G. Akhil A, Shankar AA. 2012. Toluidine blue: A review of its chemistry and clinical utility. J Oral Maxillofac Pathol 16: 251-255. PMID: 22923899
38. Surdo JL, Bauer SR. 2012. Quantitative approaches to detect donor and passage differences in adipogenic potential and clonogenicity in human bone marrow-derived mesenchymal stem cells. Tissue Eng Part C Methods 18: 877-89. PMID: 22563812
39. Suzuki S, Muneta T, Tsuji K, Ichinose S, Makino H, Umezawa A, Sekiya I. 2012. Properties and usefulness of aggregates of synovial mesenchymal stem cells as a source

for cartilage regeneration. Arthritis Research & Therapy 14:R136. PMID: 22676383
40. Tallheden T, Karlsson C, Brunner A, Tallheden T, Karlsson C, Brunner A, Van Der Lee J, Hagg R, Tommasini R, Lindahl A. 2004 Gene expression during redifferentiation of human articular chondrocytes. Osteoarthritis Cartilage 12: 525-535. PMID: 15219567
41. ten Berge D, Brugmann SA, Helms JA, Nusse R. 2008. Wnt and FGF Signals Interact to coordinate growth with cell fate specification during limb development. Development 135: 3247-3257. PMID: 18776145
42. Toh WS, Guo XM, Choo AB, Lu K, Lee EH, Cao T. 2009. Differentiation and enrichment of expandable chondrogenic cells from human embryonic stem cells in vitro. J Cell Mol Med 13: 3570-3590. PMID: 19426158
43. Truong MD, Choi BH, Kim YJ, Kim MS, Min BH. 2017. Granulocyte macrophage - colony stimulating factor (GM-CSF) significantly enhances articular cartilage repair potential by microfracture. Osteoarthritis Cartilage 25: 1345-1352 PMID: 28284999
44. Tsumaki N, Okada M, Yamashita. 2015. iPS cell technologies and cartilage regeneration. Bone 70: 48–54. PMID: 25026496
45. Twomey JD, Thakore PI, Hartman DA, Myers EGH, Hsieh AH. 2014. Roles of type VI collagen and decorin in human mesenchymal stem cell biophysics during chondrogenic differentiation. Eur Cell Mater 27: 237-250. PMID: 24668596
46. Vono R, Garcia EJ, Spinetti G, Madeddu P. 2018. Oxidative stress in mesenchymal stem cell senescence: Regulation by coding and noncoding RNAs. Antioxid Redox Signal 29: 864-879. PMID: 28762752
47. Wagner W, Horn P, Castoldi M, Diehlmann A, Bork S, Saffrich R, Benes V, Blake J, Pfister S, Eckstein V, and Ho AD. 2008. Replicative senescence of mesenchymal stem cells: a continuous and organized process. PLoS One 3: e2213.
48. Walzer SM, Toegel S, Chiari C, Farr S, Rinner B, Weinberg AM, Weinmann D, Fischer MB, Windhager R. 2019. A 3-dimensional in vitro model of zonally organized extracellular matrix. Cartilage: 1947603519865320. PMID: 31370667
49. Wang CY, Chen LL, Kuo PY, Chang JL, Wang YJ, Hung SC. 2010. Apoptosis in
50. chondrogenesis of human mesenchymal stem cells: Effect of serum and medium supplements. Apoptosis 15: 439-449. PMID: 1994997.
51. Wei Y, Zeng W, Wan R, Wang J, Zhou Q, Qiu S, Singh SR. 2012. Chondrogenic differentiation of induced pluripotent stem cells from osteoarthritic chondrocytes in alginate matrix. Eur Cell Mater 23: 1-12. PMID: 22241609
52. Yang Y, Lin H, Shen H, Wang B, Lei G, Tuan RS. 2018. Mesenchymal stem cell-derived extracellular matrix enhances chondrogenic phenotype of and cartilage formation by encapsulated chondrocytes in vitro and in vivo. Acta Biomater 69: 71-82. PMID: 29317369
53. Yelin E. 2003. The economics of osteoarthritis. In: Brandt K, Doherty M, Lohmander L, Eds., Osteoarthritis. Oxford: Oxford University Press, 2003, pp. 17-21.